Theoretical Foundations of Chemical Engineering, Vol. 33, No. 1, 1999, pp. 64–71.
Translated from Teoreticheskie Osnovy Khimicheskoi Tekhnologii, Vol. 33, No. 1, 1999, pp. 70–78.

On the Design of Microfilters

Yu. S. Polyakov, E. D. Maksimov, and V. S. Polyakov

Moscow State University of Engineering Ecology, Moscow, Russia
Institute of Medical and Biological Problems, Moscow, Russia

Received February 9, 1998

Abstract—Microfiltration is described by a mathematical model taking into account complete pore blocking, gradual pore blocking with an increase in the retentivity of the microfilter (standard blocking), primary layer (sublayer) formation, and cake formation. Membrane porosity is described by a lognormal pore-size distribution. The convexity of the kinetic curve (time divided by filtrate volume versus time) is examined for each of the elementary processes. Microfiltration kinetics are analyzed, and an approach to the design of microfilters is suggested. Theoretical estimates are compared with experimental data.

Microfiltration [1] is a complex process involving a number of simultaneous elementary processes: complete pore blocking, gradual pore blocking (termed standard blocking), primary layer (sublayer) formation, and cake formation and densification. The efficiency of crossflow microfiltration depends strongly on hydrodynamic conditions in the feed channel.

The works concerned with designing microfilters can be divided into two groups. In the first group of works [2–10], crossflow microfiltration was studied to optimize hydrodynamic conditions in the feed channel. Only filtration with cake formation (cake filtration) was considered, and the proposed models were based on the assumption that the removal rate of rejected particles from the filtering surface is proportional to the flow-velocity gradient and cake thickness [2]. Consideration was given to the situations when the removal rate is determined by shear-induced diffusion [3–5] and by the inertial lift of particles in the flow [6]. According to other models [7–10], the removal of particles from the filtering surface occurs by cake flow and rolling of particles on the cake surface along the channel. Particle flux from the filtering surface may depend on surface (double-layer, van der Waals) interactions [11]. Inertial lift of particles, convective diffusion, and free convection were also considered [11]. Generally, this group of publications [2–11] deals with steady-state microfiltration; their results are presented as a dependence of the filtration rate averaged over the channel length on the particle diameter, shear rate, particle concentration, channel length, viscosity of the liquid, etc. Note that available experimental data are often impossible to describe in terms of a single mechanism and that the exactness of the proposed models is far from acceptable [1], especially when they do not use semiempirical coefficients. Moreover, real microfiltration is an unsteady-state process, and its rate may be strongly affected by pore blocking and fouling. It is natural that these processes, leading to uncertainties in the initial conditions for calculations, may markedly decrease the exactness of prediction.

The second group of works [12–20] presents one-dimensional models of microfiltration, which qualitatively or quantitatively describe the process with the use of semiempirical coefficients. The complete pore blocking, standard blocking, and cake filtration (filtration with cake formation) models were suggested [12–16]. In these models, the volume of adsorbed particles or particles of the deposit is taken to be proportional to the filtrate volume. The analysis by Belfort *et al*. [12] was based on lognormal distribution, which agrees satisfactorily with experimental distribution data and accounts for the complexity of the process in the filter. To estimate cake growth, Suki *et al*. [17, 18] proposed an empirical expression in which the time derivative of cake weight is directly proportional to the difference between the maximum (steady-state) and current values of cake weight. As distinct from the aforementioned models [12–16], this model assumes microfiltration to be steady-state [17] and takes into account intermolecular interaction at the microporous membrane surface [18]. Earlier [19, 20], we considered the standard-blocking and surface-filtration (cake filtration) models. The standard-blocking model [19, 20], based on the assumption that the microfilter is not fouled to the full depth, assesses the effect of the pure zone on filtration kinetics, which are represented as the time dependence of time divided by filtrate volume. In the surface-filtration model [19], filtration kinetics are related to cake compressibility. The standard-blocking model [20] provided an estimate of the ratio of the fouled and free zones of a volume-action microfilter and suggested that its thickness can be reduced. The models of the second group are obviously easier to use because of their simplicity. They are more convenient in describing microfiltration when most of the coefficients involved in the first group of models are inavailable.

0040-5795/99/3301-0064$22.00 © 1999 МАИК Наука / Interperiodica Publishing

Three types of microfiltration kinetics are actually observed (Fig. 1). Curve *1*, typical for volume-action (e.g., fibrous) filters, is consistent with the model suggested by V.S. Polyakov [20]. Straight line *2* represents filtration obeying the standard-blocking model. Curve *3* was not analyzed. The assumption that the initial convexity of this curve is due to the growth of retentivity during standard blocking needs to be proven. The statement [21] that experimental-data points located to the right of the convex region also fit the standard-blocking model is not confirmed. Analysis of microfiltration kinetics, which are evidently governed by processes in the microfilter, may be very useful in developing methods for designing microfilters. The growth rate of membrane resistance as a function of resistances due to the processes involved in microfiltration [16, 22] offers a rather rough qualitative description of microfiltration. By contrast, kinetic curves both qualitatively and quantitatively characterize the process. Here, we present a mathematical model of microfiltration involving complete pore blocking, standard pore blocking (accompanied by an increase in retentivity), sublayer formation, and cake formation. Based on this model, we analyze the convexity of the microfiltration kinetic curve. We assume that the microporous membrane is characterized by a lognormal pore-size distribution.

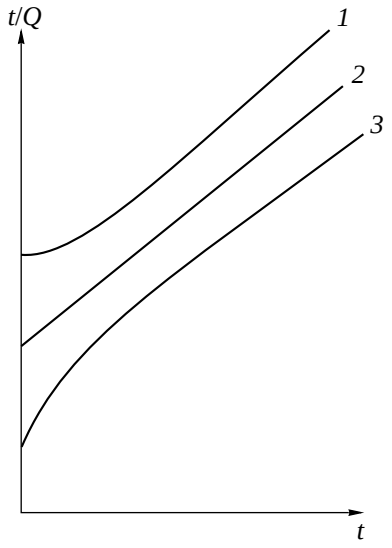

Fig. 1. Types of microfiltration kinetic curves.

MATHEMATICAL MODEL OF MICROFILTRATION

Let us consider microfiltration through a membrane with through-cylindrical pores having length l and lognormal radius distribution $N(r_0)$ [1, 23]. In general, the membrane may contain pores whose diameters are less than or equal to the diameter (d_p) of suspended particles and pores of diameters exceeding d_p. Suspended particles are taken to be rigid, spherical, and uniform in size. Let us assume that the pores of the first type will undergo complete blocking; that is, the inlet of such a pore will be completely blocked by the very first particle to arrive. The pores of the second type with $d_p < d \le k_s d_p$ ($k_s \approx 2$–20 is the cut-off coefficient accounting for surface effects and the slope of particle trajectories to the membrane surface [24]) are permeable only for the liquid. Particles, accumulating at pore inlets, first form a primary deposit layer (sublayer) [1], which is "the first brick" in the cake. Next, cake formation begins, and the membrane starts working in the surface-filtration mode. The pores of the second type with $d > k_s d_p$ first undergo standard blocking, and their retentivity increases as their free cross section diminishes because of adhesion of particles to the pore walls. When the pore diameter is decreased to $k_s d_p$, sublayer formation sets in followed by cake formation. Cake densification is not considered in this paper.

Here, we make the same assumptions as in the model proposed by V.S. Polyakov [20]: liquid flow through pores obeys the Hagen–Poiseuille equation; the volume of the particles absorbed on the inner and/or outer surface of the filter is proportional to filtrate volume; microfiltration is isothermal and occurs at a constant pressure; and the surface area of the membrane is 1 m^2.

Complete blocking. Pores with an initial radius $r_0 \le d_p/2$ undergo complete blocking. Let 1 m^3 of suspension contain n particles. The filtrate volume gained from N_{cb} pores with the radius r_0 in the period of time t will then be given by the formula [22]

$$Q_{cb} = \frac{N_{cb}}{n}\left[1 - \exp\left(-\frac{nG_{cb0}}{N_{cb}}t\right)\right], \qquad (1)$$

where

$$G_{cb0} = \frac{\pi \Delta P r_0^4}{8\mu l} N_{cb},$$

G_{cb0} is the initial rate of filtration through the pores in question.

Standard blocking. This process involves pores with $r_0 > k_s d_p/2$. For easier calculation, let the dependence of the retentivity (selectivity) R of a pore on the radius of its free cross section (r) be described by an equation similar to Ferry's steric equation [25]:

$$R = \left\{1 - \left(1 - \frac{k_s d_p}{2r}\right)^2\right\}^2.$$

From the equation

$$-2\pi l r dr = \varphi_0 \left\{1 - \left(1 - \frac{k_s d_p}{2r}\right)^2\right\}^2 dQ_{sb}$$

expressing proportionality between the volume of in-pore adsorbed particles and filtrate volume ($\varphi_0 = v_p n$ is the volume fraction of particles in the starting suspension) and the Hagen–Poiseuille law

$$\frac{dQ_{sb}}{dt} = \frac{\pi \Delta P r^4}{8\mu l},$$

we obtain the differential equation

$$\frac{dr}{dt} = -\frac{\Delta P \varphi_0}{16\mu l^2} r^3 \left[1 - \left(1 - \frac{r_{cr}}{r}\right)^2\right]^2,$$

where $r_{cr} = k_s d_p/2$. By solving the differential equations for Q_{sb} and r with the initial conditions $Q_{sb} = 0$ and $r = r_0$ at $t = 0$, we obtain expressions for calculating current and critical (corresponding to r_{cr}) values of filtrate volume and time as functions of pore radius:

$$\frac{t}{t_0} = \frac{1}{2}\left\{\frac{1}{2(r/r_{cr}) - 1} - \ln[2(r/r_{cr}) - 1]\right\} + \frac{1}{2}\left\{-\frac{1}{2(r_0/r_{cr}) - 1} + \ln[2(r_0/r_{cr}) - 1]\right\}, \quad (2)$$

$$\frac{t_{cr}}{t_0} = \frac{1}{2}\left\{1 + \ln[2(r_0/r_{cr}) - 1] - \frac{1}{2(r_0/r_{cr}) - 1}\right\}, \quad (3)$$

$$\frac{Q_{sb}}{Q_0} = -\frac{1}{8}\left\{\left(\frac{r}{r_{cr}}\right)^4 + \frac{4}{3}\left(\frac{r}{r_{cr}}\right)^3 + \frac{3}{2}\left(\frac{r}{r_{cr}}\right)^2 + 2\left(\frac{r}{r_{cr}}\right) + \frac{5}{4}\ln\left[2\left(\frac{r}{r_{cr}}\right) - 1\right] - \frac{1}{4[2(r/r_{cr}) - 1]} - \left\{\left(\frac{r_0}{r_{cr}}\right)^4 + \frac{4}{3}\left(\frac{r_0}{r_{cr}}\right)^3 + \frac{3}{2}\left(\frac{r_0}{r_{cr}}\right)^2 + 2\left(\frac{r_0}{r_{cr}}\right) + \frac{5}{4}\ln\left[2\left(\frac{r_0}{r_{cr}}\right) - 1\right] - \frac{1}{4[2(r_0/r_{cr}) - 1]}\right\}\right\}, \quad (4)$$

$$\frac{Q_{sb}^{cr}}{Q_0} = \frac{1}{8}\left\{\left(\frac{r_0}{r_{cr}}\right)^4 + \frac{4}{3}\left(\frac{r_0}{r_{cr}}\right)^3 + \frac{3}{2}\left(\frac{r_0}{r_{cr}}\right)^2 + 2\left(\frac{r_0}{r_{cr}}\right) + \frac{5}{4}\ln\left[2\left(\frac{r_0}{r_{cr}}\right) - 1\right] - \frac{1}{4[2(r_0/r_{cr}) - 1]} - \frac{67}{12}\right\}, \quad (5)$$

Sublayer formation. We assume that the hydraulic resistance of the layer of particles accumulated at the pore inlet does not noticeably affect the permeate flux until the concentration of particles at the membrane surface attains the value corresponding to the closest packing of spherical particles in the cake ($\varphi_{max} \approx 0.64$ [5]). We also assume that, within the period of time t_{cp} required for the formation of such a layer, permeate flux is determined by the hydraulic resistance of pores and remains constant. An approximate value of t_{cp} can be obtained from the formula [26]

$$\frac{\varphi_{max}}{\varphi_0} = 2 + \left(\frac{V^2 t_{cp}}{D}\right) - \left[1 + \left(\frac{V^2 t_{cp}}{2D}\right)\right]\mathrm{erfc}\left[\frac{1}{2}\sqrt{\left(\frac{V^2 t_{cp}}{D}\right)}\right] + \frac{\sqrt{(V^2 t_{cp})/D}}{\pi}\exp\left[-\frac{1}{4}\left(\frac{V^2 t_{cp}}{D}\right)\right], \quad (6)$$

where

$$\mathrm{erfc}(X) = \frac{2}{\sqrt{\pi}}\int_X^\infty \exp(-u^2)du,$$

V is the mean integral permeate velocity taking into account pore-size distribution and the porosity of the membrane, and D is the diffusion coefficient of particles in the suspension. The value of D is estimated from the Einstein formula [27] or from the expression for shear-induced diffusion [1, 5]. The assumption that the permeate flux is constant during sublayer formation is confirmed by calculations using the expression for pressure drop accross the concentration polarization layer at the membrane surface [28]:

$$\Delta P_{cp} = \frac{3kT}{4\pi\left(\frac{d_p}{2}\right)^3}\int_0^{\varphi_{max}^{1/3}} A_s(\theta) 3\theta^2 d\theta,$$

where

$$A_s(\theta) = \frac{1 + \frac{2}{3}\theta^5}{1 - \frac{3}{2}\theta + \frac{3}{2}\theta^5 - \theta^6}.$$

Cake formation. Once a sublayer is formed, surface filtration begins. The initial resistance to surface filtration is equal to membrane resistance. The filtrate volume gained from a membrane surface area containing one pore is given by the expression [22]:

$$\frac{Q_{cf,i}}{Q_0} = \frac{1}{\beta}\left\{\sqrt{a_i^2 + 2\beta\frac{t_{cf}}{t_0}} - a_i\right\}, \quad (7)$$

where

$$a_i = \begin{cases} \int_{\rho_p}^1 N(\rho_0)d\rho_0 \Big/ \left(\int_{\rho_p}^1 \rho_0^4 N(\rho_0)d\rho_0\right) & i = 1, \\ 1 & i = 2; \end{cases}$$

$$\beta = \frac{\pi^2 r_c N_0^2 r_{cr}^6}{8S^2};$$

$r_c = \alpha/d_p^2$ is the specific hydraulic resistance of the cake [29]; N_0 is the total number of pores; S is the surface area of the membrane; $i = 1$ corresponds to the resistance of the membrane portion with $d_p/2 < r_0 < r_{cr}$; and $i = 2$ corresponds to the case of $r_0 > r_{cr}$.

Equations (1)–(7) enable us to create an algorithm for calculating microfiltration parameters that takes into account the initial pore-size distribution.

Let us introduce the following dimensionless parameters:

$$q_{cb} = Q_{cb}/Q_0, \quad q_{sb} = Q_{sb}/Q_0, \quad q_{sub} = Q_{sub}/Q_0,$$
$$q_{cf} = Q_{cf}/Q_0, \quad \tau = t/t_0, \quad \tau_{cr} = t_{cr}/t_0,$$
$$\tau_{cp} = t_{cp}/t_0, \quad \rho = r/r_{cr}, \quad \rho_0 = r_0/r_{cr},$$
$$\rho_p = d_p/(2r_{cr}), \quad A = 1/(nQ_0), \quad \eta = V^2 t_0/D.$$

In the dimensionless form, equations (1)–(7) appear as

$$q_{cb} = AN_{cb}[1 - \exp(-\rho_0^4 \tau/A)], \tag{8}$$

$$\tau = \frac{1}{2}\left\{\frac{1}{2\rho - 1} - \ln[2\rho - 1]\right\} + \frac{1}{2}\left\{-\frac{1}{2\rho_0 - 1} + \ln[2\rho_0 - 1]\right\}, \tag{9}$$

$$\tau_{cr} = \frac{1}{2}\left\{1 + \ln[2\rho_0 - 1] - \frac{1}{2\rho_0 - 1}\right\}, \tag{10}$$

$$q_{sb} = -\frac{1}{8}\left\{\rho^4 + \frac{4}{3}\rho^3 + \frac{3}{2}\rho^2 + 2\rho + \frac{5}{4}\ln[2\rho - 1] - \frac{1}{4[2\rho - 1]} - \left\{\rho_0^4 + \frac{4}{3}\rho_0^3 + \frac{3}{2}\rho_0^2 + 2\rho_0 + \frac{5}{4}\ln[2\rho_0 - 1] - \frac{1}{4[2\rho_0 - 1]}\right\}\right\}, \tag{11}$$

$$q_{sb}^{cr} = \frac{1}{8}\left\{\rho_0^4 + \frac{4}{3}\rho_0^3 + \frac{3}{2}\rho_0^2 + 2\rho_0 + \frac{5}{4}\ln[2\rho_0 - 1] - \frac{1}{4[2\rho_0 - 1]} - \frac{67}{12}\right\}, \tag{12}$$

$$\frac{\varphi_{max}}{\varphi_0} = 2 + \eta\tau_{cp} - \left[1 + \frac{\eta\tau_{cp}}{2}\right]\mathrm{erfc}\left[\frac{1}{2}\sqrt{\eta\tau_{cp}}\right] + \frac{\sqrt{\eta\tau_{cp}}}{\pi}\exp\left[-\frac{1}{4}\eta\tau_{cp}\right], \tag{13}$$

$$q_{cf,i} = \frac{1}{\beta}\{\sqrt{a_i^2 + 2\beta\tau_{cf}} - a_i\}. \tag{14}$$

Let us write the probability density function for lognormal pore-size distribution as [23]

$$f(\rho_0) = \frac{1}{\rho_0\sqrt{2\pi}}[\ln(1 + (\rho_\sigma/\rho^*)^2)]^{-1/2} \times \exp\left\{-\frac{[\ln(\rho_0\sqrt{1 + (\rho_\sigma/\rho^*)^2}/\rho^*)]^2}{2\ln(1 + (\rho_\sigma/\rho^*)^2)}\right\},$$

where

$$\rho_l = r_l/r_{cr}, \quad \rho_{up} = r_{up}/r_{cr},$$
$$\rho^* = r^*/r_{cr}, \quad \rho_\sigma = r_\sigma/r_{cr}.$$

The number of pores with radius ρ_0 is given by

$$N(\rho_0) = n_0 f(\rho_0), \tag{15}$$

where

$$n_0 = N_0/\left(\int_{\rho_l}^{\rho_{up}} f(\rho_0)d\rho_0\right).$$

For microfiltration time τ, contributions from different types of pores to the filtrate volume can be calculated by the formulas presented below. We consider the general case, that is, the case where the membrane contains all three types of pores:

1) $\rho_0 \le \rho_p$

$$q_{cb}^{\Sigma} = A\int_{\rho_l}^{\rho_p}[1 - \exp(-\rho_0^4\tau/A)]N(\rho_0)d\rho_0; \tag{16}$$

2) $\rho_p < \rho_0 \le 1$

for $\tau \le \tau_{cp}$

$$q_{sub}^{\Sigma} = \tau\int_{\rho_p}^{1}\rho_0^4 N(\rho_0)d\rho_0; \tag{17}$$

for $\tau > \tau_{cp}$

$$q_{sub}^{\Sigma} = \tau_{cp}\int_{\rho_p}^{1}\rho_0^4 N(\rho_0)d\rho_0 + \frac{1}{\beta}[\sqrt{a_1^2 + 2\beta(\tau - \tau_{cp})} - a_1]\int_{\rho_p}^{1}N(\rho_0)d\rho_0; \tag{18}$$

3) $\rho_0 > 1$

for $\tau \le \tau_{cp}$

$$q_{sb}^{\Sigma} = \int_{1}^{\rho_{01}} q_{sb}^{cr} N(\rho_0) d\rho_0 + \int_{\rho_{01}}^{\rho_{up}} q_{sb} N(\rho_0) d\rho_0 + \int_{1}^{\rho_{01}} (\tau - \tau_{cr}) N(\rho_0) d\rho_0; \quad (19)$$

for $\tau > \tau_{cp}$

$$q_{sb}^{\Sigma} = \int_{1}^{\rho_{01}} q_{sb}^{cr} N(\rho_0) d\rho_0 + \int_{\rho_{01}}^{\rho_{up}} q_{sb} N(\rho_0) d\rho_0 + \int_{\rho_{02}}^{\rho_{01}} (\tau - \tau_{cr}) N(\rho_0) d\rho_0 + \tau_{cp} \int_{1}^{\rho_{02}} N(\rho_0) d\rho_0 + \frac{1}{\beta} \int_{1}^{\rho_{02}} [\sqrt{a_2^2 + 2\beta(\tau - \tau_{cp} - \tau_{cr})} - a_2] N(\rho_0) d\rho_0. \quad (20)$$

The value of ρ_{01} can be found from equation (10) with τ instead of τ_{cr}; q_{sb}, as a function of τ and ρ_0, is determined from equations (9) and (11). The value of ρ_{02} is obtained by solving the equation

$$\frac{1}{2}\left\{1 + \ln[2\rho_{02} - 1] - \frac{1}{2\rho_{02} - 1}\right\} = \tau - \tau_{cp}. \quad (21)$$

After summation of the filtrate volumes gained from all types of pores, we can calculate the microfiltration kinetic curve.

Let us write the equations of kinetic curves for elementary processes involved in microfiltration and analyze the convexities of the curves.

Complete blocking. By dividing τ by expression (16) and taking the second time derivative of the resulting expression, we obtain

$$\left(\frac{\tau}{q_{cb}}\right)'' = \frac{2(q_{cb}')^2\tau - 2q_{cb}'q_{cb} - q_{cb}''q_{cb}\tau}{q_{cb}^3},$$

where

$$q_{cb}' = \int_{\rho_l}^{\rho_p} \rho_0^4 \exp(-\rho_0^4\tau/A) N(\rho_0) d\rho_0,$$

$$q_{cb}'' = -\frac{1}{A}\int_{\rho_l}^{\rho_p} \rho_0^8 \exp(-\rho_0^4\tau/A) N(\rho_0) d\rho_0.$$

Numerical analysis of the second derivative with the use of the Mathematica 3.0 program [30] shows that the initial small portion of the curve is slightly convex. As τ increases, the second derivative tends to zero and the kinetic curve flattens to a straight line.

Standard blocking. In this case,

$$\left(\frac{\tau}{q_{sb}}\right)'' = \frac{2(q_{sb}')^2\tau - 2q_{sb}'q_{sb} - q_{sb}''q_{sb}\tau}{q_{sb}^3},$$

where

$$q_{sb}' = \rho^4, \quad q_{sb}'' = -2\rho^2(2\rho - 1)^2,$$

as well as τ and q_{sb}, is given by expressions (9) and (11). Numerical analysis shows that the second derivative is positive in the range $1 < \rho_0 < 1000$. Therefore, the kinetic curve for this elementary process is convex downwards (concave) in all practical cases.

Sublayer formation. In this case, the kinetic curve is described by the equation

$$\tau/q_{sub,\,i} = \tau/(I_i(\tau - \tau_i) + q_i),$$

where

$$I_i = \begin{cases} \rho_0^4, & i = 1, \\ 1, & i = 2; \end{cases}$$

$$q_i = \begin{cases} 0, & i = 1, \\ q_{sb}^{cr}, & i = 2; \end{cases}$$

$$\tau_i = \begin{cases} 0, & i = 1, \\ \tau_{cr}, & i = 2. \end{cases}$$

The second derivative

$$\left(\frac{\tau}{q_{sub,\,i}}\right)'' = -\frac{2I_i(q_i - I_i\tau_i)}{[I_i(\tau - \tau_i) + q_i]^3}$$

is negative or, at $i = 1$, zero, as is the first derivative. Therefore, the kinetics of this elementary process are described by a convex curve or a straight line parallel to the abscissa axis.

Cake formation. The kinetic curve relevant to this process is given by

$$\frac{\tau}{q_{cf,\,i}} = \frac{\tau}{\frac{1}{\beta}\{\sqrt{a_i^2 + 2\beta(\tau - \tau_{cp} - \tau_i)} - a_i\} + I_i\tau_{cp} + q_i}.$$

The second derivative of this equation is

$$\left(\frac{\tau}{q_{cf,\,i}}\right)'' = \beta^2\{2a_i^3 - 2a_i^2[\beta(q_i + I_i\tau_{cp}) + m_i] + a_i\beta[3\tau - 4(\tau_{cp} + \tau_i)] + \beta[\beta(q_i + I_i\tau_{cp}) \times (-3\tau + 4(\tau_{cp} + \tau_i)) + m_i(-\tau + 4(\tau_{cp} + \tau_i))]\}/[m_i(-a_i + \beta(q_i + I_i\tau_{cp}) + m_i)]^3,$$

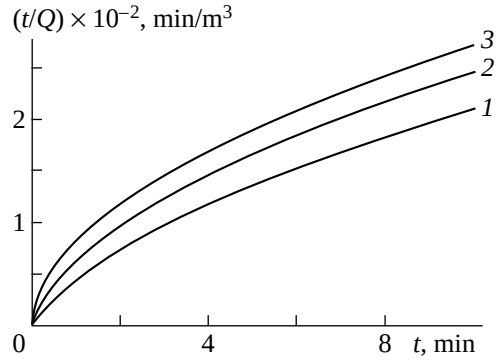

Fig. 2. t/Q versus time: k_s = (*1*) 6, (*2*) 9, (*3*) 12; β = (*1*) 1.81, (*2*) 20.67, (*3*) 116.13; t_{cp} = (*1*) 0.04, (*2*) 0.011, (*3*) 0.006 s; $l = 28.2 \times 10^{-6}$ m; $d_p = 2.2 \times 10^{-8}$ m; $r^* = 1.1 \times 10^{-7}$ m; $r_{up} = 1.83 \times 10^{-7}$ m; $r_l = 5.96 \times 10^{-8}$ m; $\sigma = 2.57 \times 10^{-8}$ m; $n_0 = 1.6 \times 10^{13}$.

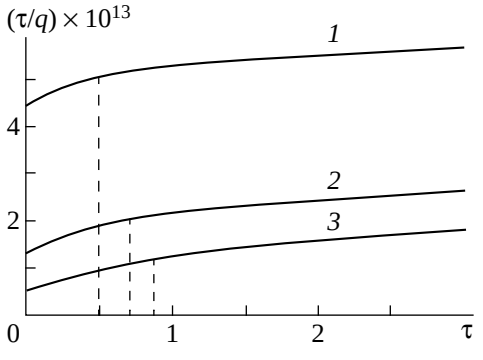

Fig. 3. τ/q versus dimensionless time: ρ* = (*1*) 0.7, (*2*) 1.0, (*3*) 1.3; ρ_l = (*1*) 0.24, (*2*) 0.54, (*3*) 0.84; ρ_{up} = (*1*) 1.37, (*2*) 1.67, (*3*) 1.97; τ_{cp} = (*1*) 1.3×10^{-2}, (*2*) 4.0×10^{-3}, (*3*) 9.0×10^{-4}; $d_p = 2.93 \times 10^{-8}$ m; k_s = 7.5; β = 0.349; ρ_σ = 0.23; $n_0 = 5.95 \times 10^{12}$.

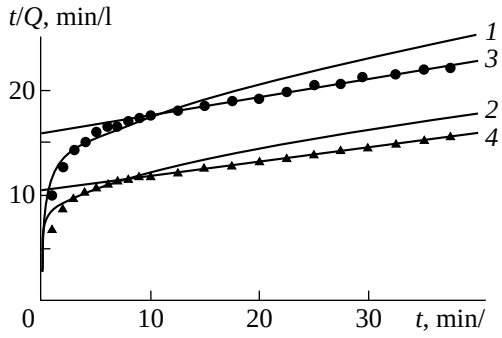

Fig. 4. Time dependence of $t/_Q$ for crossflow microfiltration: ΔP = (*1*) 3.8, (*2*) 4.85 kPa; β = (*1*) 0.044, (*2*) 0.031; l = (*1*) 1.0×10^{-5}, (*2*) 8.23×10^{-6} m; t_{cp} = (*1*) 0.58, (*2*) 0.23 s; $r_0 = 1.0 \times 10^{-7}$ m; k_s = 12.8; $N_0 = 2.29 \times 10^{11}$. Lines *1* and *2* represent model (1)–(7); lines *3* and *4*, standard-blocking model [21]; points, experimental data [21].

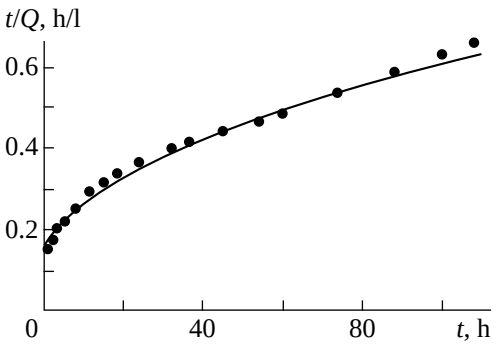

Fig. 5. Time dependence of $t/_Q$ for a radial metal-ceramic microfilter: $l = 1.6 \times 10^{-3}$ m, $r_l = 4.88 \times 10^{-8}$ m, $r_{up} = 1.35 \times 10^{-7}$ m, $r^* = 9.0 \times 10^{-8}$ m, $\sigma = 2.1 \times 10^{-8}$ m, β = 23.73, k_s = 9, $d_p = 2.7 \times 10^{-8}$ m, t_{cp} = 3680 s; $n_0 = 1.17 \times 10^{13}$. The line represents our model; points, experimental data [32].

where

$$m_i = \sqrt{a_i^2 + 2\beta(\tau - \tau_{cp} - \tau_i)}.$$

This second derivative is negative during cake formation except for a short period of time at the beginning of the process (the cumbersome expression determining this period is not presented here).

Thus, we found that the convex portion of curve *3* (Fig. 1) is only due to cake formation on the membrane surface. Therefore, attempts to describe either the convex or adjacent portions of the kinetic curve by the standard-blocking model [21; 24, p. 112] are in conflict with the physics of crossflow microfiltration.

RESULTS AND DISCUSSION

Calculations illustrating the effect of microfiltration parameters on the shape of the kinetic curve were carried out for an SM (Millipore) membrane with an effective pore diameter of 0.22 μm and a distilled-water permeability of 2.5×10^{-3} m^3/(m^2 s) at 7.7×10^{-4} Pa and room temperature [32].

It was found that the convexity of the kinetic curve is most affected by k_s in addition to the ratio of pore size and critical radius (Figs. 2, 3). The convexity grows with an increasing k_s and decreasing ρ* (except for the region where the mean radius is much smaller than ρ_p). The dimensionless time necessary for sublayer formation is several orders less than the critical time for standard blocking of pores with the radius r_{up}. As would be expected, complete blocking exerts no noticeable effect on the kinetic curve for the overall process if the membrane contains a considerable proportion of pores with a radius larger than $d_p/2$. The specific resistance of the cake layer (r_c) most strongly affects the shape of the curve in the region to the right of the most convex portion.

The proposed algorithm was used in processing earlier reported experimental data [21, 32]. Visvanathan and Ben Aim [21] studied crossflow microfiltration in a plane-cell unit with a Gelman Science Versapore-200

membrane (effective pore size is 0.2 μm; membrane surface, 80 cm^2; particle diameter, 12 nm; suspension velocity, 0.5 m/s; particle concentration, 1 g/l). The results of the calculations are presented in Fig. 4. One can see that our model is consistent with experimental data. The deviation of our calculated curves from data points at great values of t is explained by the fact that the crossflow membrane unit turns to the steady-state operation in the course of time, while our model was suggested for unsteady-state conditions only. It is evident that the standard-blocking model [21] (straight lines *3* and *4*), though consistent with experimental data to the right of the convex region, is not valid for the whole process.

Long-term experiments on the purification of bath water were performed in the Institute of Medical and Biological Problems [32]. Water contaminated by detergents (synthetic surfactants), as well as with suspended and colloidal particles that were washed off human bodies, was passed through a microfiltration unit. The filtrate was fed into a reverse-osmosis device and, next, into an adsorption finish purifier. The microfilter used in the experiments was radial and had a porous metalloceramic membrane with supported silica gel. Water contained 1 g/l of suspended and colloidal impurities. The retentivity of the filter was close to 100%. The static pressure drop in the filter was maintained at 0.02 MPa. The membrane surface area was 35 dm^2. The filtration rate was measured with the use of 100- and 500-ml measuring cylinders and a stopwatch to within an accuracy of 3% or better.

Microfiltration kinetic data are presented in Fig. 5. Coefficients for the model were found from experimental data points. As is seen from Fig. 5, theoretical curves fit experimental data reasonably well.

Thus, the mathematical model presented here adequately describes real microfiltration processes and can be used in designing microfilters.

NOTATION

d_p—diameter of particles in suspension, m;

D—diffusion coefficient, m^2/s;

G_{cb0}—initial permeate flux through the pores with a radius $r_0 \le d_p/2$, m^3/s;

k—Boltzmann constant, J/K;

k_s—cut-off coefficient;

l—pore length, m;

n—number of particles in 1 m^3 of suspension, m^{-3};

$N(r_0)$—number of pores with radius r_0 per 1 m^2 of the membrane (lognormal distribution), m^{-1};

ΔP—pressure drop across the membrane, Pa;

ΔP_{cp}—pressure drop across the concentration polarization layer, Pa;

q—dimensionless filtrate volume;

q_{cb}^{Σ}—diomensionless filtrate volume gained from the pores with $\rho_0 \le \rho_p$;

q_{sub}^{Σ}—diomensionless filtrate volume gained from the pores with $\rho_p < \rho_0 \le 1$;

q_{sb}^{Σ}—diomensionless filtrate volume gained from the pores with $\rho_0 > 1$;

Q—filtrate volume, m^3;

r—pore radius, m;

r_c—specific resistance of the cake layer, m^{-2};

r_l—lower limit of the initial pore radius, m;

r_0—initial pore radius, m;

r_{up}—upper limit of the initial pore radius, m;

r^*—mean value for $N(r_0)$, m;

R—selectivity;

R_m—membrane resistance, m^{-1};

S—membrane surface area, m^2;

T—temperature, K;

t—time, s;

v_p—particle volume, m^3;

φ—volume fraction of particles in suspension;

μ—dynamic viscosity coefficient, Pa s;

ρ—dimensionless pore radius;

ρ_l—lower limit of the dimensionless initial pore radius;

ρ_0—dimensionless initial pore radius;

ρ_{up}—upper limit of the dimensionless initial pore radius;

ρ_σ—dimensionless standard deviation for the lognormal distribution $N(\rho_0)$;

ρ^*—dimensionless mean (dimensionless mean radius) for $N(\rho_0)$;

σ—standars deviation for $N(\rho_0)$, m;

τ—dimensionless time.

SUBSCRIPTS

0—initial value;

cb—complete blocking;

cf—cake formation;

cr—critical value;

sb—standard blocking;

sub—sublayer formation.

REFERENCES

1. Belfort, G., Davis, R.H., and Zydney, A.L., The Behavior of Suspensions and Macromolecular Solutions in Cross-Flow Microfiltration, *J. Membr. Sci*., 1994, vol. 96, p. 1.

2. Shulz, G. and Ripperger, S., Concentration Polarization in Crossflow Microfiltration, *J. Membr. Sci*., 1989, vol. 40, p. 173.
3. Zydney, A.L. and Colton, S.K., A Concentration Polarization Model for the Filtrate Flux in Crossflow Microfiltration of Particulate Suspensions, *Chem. Eng. Commun.*, 1986, vol. 47, p. 1.
4. Davis, R.H. and Sherwood, J.D., A Similarity Solution for Steady-State Crossflow Microfiltration, *Chem. Eng. Commun.*, 1990, vol. 45, p. 3204.
5. Romero, C.A. and Davis, R.H., Transient Model of Crossflow Microfiltration, *Chem. Eng. Sci*., 1990, vol. 45, p. 13.
6. Belfort, G., Fluid Mechanics in Membrane Filtration: Recent Developments, *J. Membr. Sci*., 1989, vol. 40, p. 123.
7. Davis, R.H. and Birdsell, S.A., Hydrodynamic Model and Experiments for Crossflow Microfiltration, *Chem. Eng. Commun.*, 1987, vol. 49, p. 217.
8. Leonard, E.G. and Vassilieff, C.S., The Deposition of Rejected Matter in Membrane Separation Processes, *Chem. Eng. Commun.*, 1984, vol. 30, p. 209.
9. Stamatakis, K. and Tien, C., A Simple Model of Crossflow Filtration Based on Particle Adhesion, *AIChE J.*, 1993, vol. 39, p. 1293.
10. Sherwood, J.D., The Force on a Sphere Pulled away from a Permeable Half-Space, *Physicochem. Hydrodynamics*, 1988, vol. 10, p. 3.
11. Song, L. and Elimelech, M., Particle Deposition onto a Permeable Surface in Laminar Flow, *J. Colloid Interface Sci.*, 1995, vol. 173, p. 165.
12. Belfort, G., Pimbley, J.M., Greiner, A., and Chung, K.-Y., Diagnosis of Membrane Fouling Using Rotating Annular Filter, *J. Membr. Sci*., 1993, vol. 77, p. 1.
13. Chandavarkar, A.S., Dynamics of Fouling of Microporous Membranes by Proteins, *Doctoral Dissertation*, Cambridge (MA): Mass. Inst. of Technol., 1990.
14. Bowen, W.R. and Gan, Q., Properties of Microfiltration Membranes: Flux Loss during Constant Pressure Permeation of Bovine Serum Albumim, *Biotechnol. Bioeng.*, 1991, vol. 38, p. 688.
15. Bowen, W.R. and Gan, Q., Properties of Microfiltration Membranes: the Effects of Adsorption and Shear on the Recovery of an Enzyme, *Biotechnol. Bioeng.*, 1992, vol. 40, p. 491.
16. Bowen, W.R., Calvo, J.I., and Hernandez, A., Steps of Membrane Blocking in Flux Decline during Protein Microfultration, *J. Membr. Sci*., 1995, vol. 101, p. 153.
17. Suki, A., Fane, A.G., and Fell, C.J.D., Flux Decline in Protein Ultrafiltration, *J. Membr. Sci*., 1984, vol. 21, p. 269.
18. Suki, A., Fane, A.G., and Fell, C.J.D., Modelling Fouling Mechanisms in Protein Ultrafiltration, *J. Membr. Sci*., 1986, vol. 27, p. 181.
19. Polyakov, S.V., Maksimov, E.D., and Polyakov, V.S., On the Simulation of One-Dimensional Microfiltration, *Teor. Osn. Khim. Tekhnol*., 1995, vol. 29, no. 4, p. 357.
20. Polyakov, V.S., The Design of a Positive-Displacement Filter, *Teor. Osn. Khim. Tekhnol.*, 1998, vol. 32, no. 1, p. 22.
21. Visvanathan, C. and Ben Aim, R., Studies on Colloidal Membrane Fouling Mechanisms in Crossflow Microfiltration, *J. Membr. Sci*., 1989, vol. 45, p. 3.
22. Zhuzhikov, V.A., *Fil'trovanie: Teoriya i praktika razdeleniya suspenzii* (Filtration of Suspensions: Theory and Practice), Moscow: Khimiya, 1980.
23. Zydney, A.L., Aimar, P., and Meireles, M., Use of the Lognormal Probability Density Function to Analyze Membrane Pore Size Distributions: Functional Forms and Discrepancies, *J. Membr. Sci*., 1994, vol. 91, p. 293.
24. Bryk, M.T. and Tsapyuk, E.A., *Ul'trafil'tratsiya* (Ultrafiltration), Kiev: Naukova Dumka, 1989.
25. Nakano, S., Determination of Pore Size and Pore Size Distribution: 3. Filtration Membranes (Review), *J. Membr. Sci*., 1994, vol. 96, p. 131.
26. Nakano, Y., Tien, C., and Gill, W.N., Nonlinear Convective Diffusion: A Hyperfiltration Application, *AIChE J.*, 1967, vol. 13, p. 1092.
27. Elimelech, M., Gregory, J., Jia, X., and Williams, R., *Particle Deposition and Aggregation: Measurement, Modelling, and Simulation*, Oxford: Butterworth-Heinemann, 1995.
28. Song, L. and Elimelech, M., Theory of Concentration Polarization in Crossflow Filtration, *J. Chem. Soc., Faraday Trans.*, 1995, vol. 91, p. 3389.
29. Polyakov, V.S., Maksimov, E.D., and Polyakov, S.V., Simulation of Cross-Flow Microfiltration, *Teor. Osn. Khim. Tekhnol.*, 1995, vol. 29, no. 3, p. 300.
30. Wolfram, S., *Mathematica: A System for Doing Mathematics by Computer*, Redwood City: Addison–Wesley, 1991.
31. Dubyaga, V.P., Perechkin, L.P., and Katalevskii, E.E., *Polimernye membrany* (Polimeric Membranes), Moscow: Khimiya, 1981.
32. Polyakov, S.V., Volgin, V.D., Sinyak, Yu.S., *et al*., Back-Osmosis Regeneration of Sanitary-and-Hygienic Water for Long-Term Space Flights, *Kosm. Biol. Aviokosm. Med.*, 1986, no. 2, p. 78.

SPELLING:
accross
surfactants
diomensionless
standars
Albumim
Microfultration
Aviokosm